New Phytologist

Research

A gene regulatory network critical for axillary bud dormancy directly controlled by Arabidopsis BRANCHED1

Sam W. van Es[1,2]*, Aitor Muñoz-Gasca[3]*, Francisco J. Romero-Campero[4,5], Eduardo González-Grandío[3], Pedro de los Reyes[4], Carlos Tarancón[3], Aalt D. J. van Dijk[6], Wilma van Esse[1,2], Alberto Pascual-García[7], Gerco C. Angenent[1,2], Richard G. H. Immink[1,2] and Pilar Cubas[3]

[1]Bioscience, Wageningen Plant Research, Wageningen University & Research, 6708 PB, Wageningen, the Netherlands; [2]Laboratory of Molecular Biology, Wageningen University & Research, 6708 PB, Wageningen, the Netherlands; [3]Department of Plant Molecular Genetics, Centro Nacional de Biotecnología/Consejo Superior de Investigaciones Científicas, Campus Universidad Autónoma de Madrid, 28049, Madrid, Spain; [4]Institute for Plant Biochemistry and Photosynthesis, Universidad de Sevilla – Consejo Superior de Investigaciones Científicas, Ave. Américo Vespucio 49, 41092, Seville, Spain; [5]Department of Computer Science and Artificial Intelligence, Universidad de Sevilla, Ave. Reina Mercedes s/n, 41012, Seville, Spain; [6]Bioinformatics, Wageningen University & Research, 6708 PB, Wageningen, the Netherlands; [7]Department of Systems Biology, Centro Nacional de Biotecnología/Consejo Superior de Investigaciones Científicas, Campus Universidad Autónoma de Madrid, 28049, Madrid, Spain

Authors for correspondence:
Pilar Cubas
Email: pcubas@cnb.csic.es

Richard G. H. Immink
Email: richard.immink@wur.nl

Received: *22 April 2023*
Accepted: *21 October 2023*

New Phytologist (2024) **241:** 1193–1209
doi: 10.1111/nph.19420

Key words: Arabidopsis, axillary bud dormancy, *BRANCHED1*, gene regulatory network, shoot branching, systems biology, TCP, transcription factors.

Summary

- The *Arabidopsis thaliana* transcription factor BRANCHED1 (BRC1) plays a pivotal role in the control of shoot branching as it integrates environmental and endogenous signals that influence axillary bud growth. Despite its remarkable activity as a growth inhibitor, the mechanisms by which BRC1 promotes bud dormancy are largely unknown.
- We determined the genome-wide BRC1 binding sites *in vivo* and combined these with transcriptomic data and gene co-expression analyses to identify *bona fide* BRC1 direct targets. Next, we integrated multi-omics data to infer the BRC1 gene regulatory network (GRN) and used graph theory techniques to find network motifs that control the GRN dynamics. We generated an open online tool to interrogate this network. A group of BRC1 target genes encoding transcription factors (BTFs) orchestrate this intricate transcriptional network enriched in abscisic acid-related components.
- *Promoter::β-GLUCURONIDASE* transgenic lines confirmed that BTFs are expressed in axillary buds. Transient co-expression assays and studies *in planta* using mutant lines validated the role of BTFs in modulating the GRN and promoting bud dormancy.
- This knowledge provides access to the developmental mechanisms that regulate shoot branching and helps identify candidate genes to use as tools to adapt plant architecture and crop production to ever-changing environmental conditions.

Introduction

In multicellular organisms, growth and development occur by the sequential activation of gene regulatory networks (GRNs) that influence patterns of cell division and differentiation, which results in species-specific morphologies. Sessile organisms, such as plants, need to adapt these developmental programmes to environmental conditions and resource availability. Thus, the activity of GRNs, controlled by transcriptional master regulators, is modulated by external signals, such as light quality, photoperiod and temperature and endogenous cues that signal stress and nutrient and energy availability.

In higher plants, one key developmental programme that determines aboveground plant architecture is the formation of branches, lateral shoots derived from axillary buds. Under favourable conditions, axillary buds continue to grow out and elongate. However, under actual or potential energy-limiting situations, the buds remain small and dormant in the leaf axils (Martín-Fontecha *et al.*, 2018). Thus, axillary bud activity is strongly influenced by environmental cues, sugar availability and hormonal signals that move through the plant (Wang *et al.*, 2019). However, the molecular genetic mechanisms that integrate these signals inside the axillary buds and implement the responses leading to growth arrest or activation are still poorly understood.

In *Arabidopsis thaliana*, *BRANCHED1* (*BRC1*) is a central local regulator of bud activity that encodes a TEOSINTE BRANCHED1, CYCLOIDEA, PCF (TCP; Cubas *et al.*, 1999) transcription factor (TF), whose function is widely conserved in angiosperms. *BRC1* and its orthologues are expressed in axillary buds and promote growth arrest: *brc1* mutants have

*These authors contributed equally to this work.

constitutively active buds, and therefore excessive branching, in a wide variety of species (Wang *et al.*, 2019). Due to the spatially restricted expression patterns of *BRC1*, limited to axillary buds, this gene only prevents lateral branching. However, when ectopically expressed in Arabidopsis seedlings, it causes growth arrest of the shoot and root apical meristems and leaf primordia (González-Grandío *et al.*, 2013). In hybrid aspen, *BRC1*-like genes, expressed in the shoot apex in short days, promote apical growth cessation (Maurya *et al.*, 2020). Despite all these remarkable growth-inhibiting effects of *BRC1* and its major role in the control of plant architecture, the gene targets and GRNs controlled directly by BRC1 remain largely unknown in Arabidopsis. Three closely related Homeodomain-Leucine Zipper-I (HD-zip-I) genes (*HOMEOBOX (HB)21*, *HB40* and *HB53*) are direct BRC1 targets and mediate *BRC1*-induced abscisic acid (ABA) synthesis and response in buds. ABA signalling in turn promotes inhibition of bud growth (González-Grandío *et al.*, 2017). Furthermore, two clusters of co-expressed genes (one enriched in genes related to cell division and DNA replication, another in chloroplast and ribosomal genes) are downregulated in response to *BRC1*, although it is unclear whether this control is direct (González-Grandío *et al.*, 2013). In maize, the closely related TCP factor Teosinte Branched1 (TB1) directly influences hormone signalling (ABA, gibberellic acid (GA) and jasmonate (JA)) and sugar signalling (Dong *et al.*, 2019). However, it is unclear how conserved the targets of TB1 and Arabidopsis BRC1 are, as there is abundant evidence of the divergent regulatory pathways associated with *TB1* and *BRC1*.

In this work, we have characterised the transcriptional GRN that operates directly downstream of Arabidopsis BRC1 to promote axillary bud growth arrest. For this, we subjected transcriptomic data from active and dormant axillary buds to co-expression analyses. Then, we compared this data with the transcriptome obtained from seedlings shortly after *BRC1* induction and with the *in vivo* genome-wide binding sites of BRC1 elucidated from chromatin immunoprecipitation sequencing (ChIP-Seq). We integrated these and additional omics data to infer the BRC1 GRN, and used graph theory techniques applied in systems biology to identify significant network motifs. This GRN is enriched in feed-forward loops (FFLs) and feedback loops (FBLs), and is highly redundant, which probably confers robustness against noise and mutation. To explore the network properties further, we developed an open interactive web application, BRC1NET. All these studies allowed us to identify a group of direct targets of BRC1 encoding TFs that we termed BTFs, which play critical roles in the regulation of the network.

As a biological confirmation of the data obtained, we performed *in planta* experiments that indicate that BTFs coordinate, together with BRC1, this intricate GRN enriched in ABA signalling components. First, *promoter::β-GLUCURONIDASE (promoter::GUS)* transgenic lines confirmed the localised expression of the BTFs in axillary buds like that of *BRC1*. Second, transient co-expression assays validated the role of some of these BTFs in the co-regulation of BRC1 targets and support that they fine-tune the transcriptional responses in cooperation with BRC1. Finally, the wild-type (WT) or mild branching phenotypes of BTF single mutant lines support the robustness of the network to mutation predicted by our model. This knowledge provides access to the regulatory mechanisms that control shoot branching and will aid in identifying genetic tools to adapt plant architecture to limiting environmental conditions.

Materials and Methods

Plant materials and growth condition

Wild-type *Arabidopsis thaliana* Columbia-0 (Col-0), the *brc1-2* mutant and the oestradiol-inducible *GREEN FLUORESCENCE PROTEIN::BRC1* lines in a *brc1-2* background (*LEXA::GFP::BRC1*^{ind}; *brc1-2* or *GFP::BRC1*^{ind} for short) were used (Aguilar-Martínez *et al.*, 2007; González-Grandío *et al.*, 2017). The *abf3-cr1* line is a crispr mutant generated in Cubas' Lab that has a 1-base pair (bp) deletion at position 572 of the *ABF3* coding sequence, which renders a truncated protein of 196 amino acids instead of the 454 amino acid-long WT ABF3 protein. The *abi5-8* mutant, provided by Prof. Oscar Lorenzo, was described in Zheng *et al.* (2012). All lines were grown in soil or *in vitro* in ½ Murashige & Skoog (½MS) medium 1% (w/v) agar plates under long-day conditions (16 h : 8 h, light : dark cycle) at 21°C in white light (PAR 120 µmol m^{-2} s^{-1}). For short-day experiments, plants were grown in the same conditions, but with 8 h : 16 h, light : dark.

Phenotypic analyses

abi5-8 and *abf3-cr1* mutant plants were grown for 1 month under short-day photoperiod (8 h : 16 h, light : dark) and then were transferred to long-day photoperiod (16 h : 8 h, light : dark). After flowering, the main shoot was decapitated and 2 wk later the number of rosette branches was counted.

Plasmid generation

For *promoter::GUS* constructs, genomic fragments of 1728, 1709, 1830, 2265, 1846, 540 and 1990 bp comprising the BRC1 binding peaks upstream the translation start codon ATG of *ABA INSENSITIVE 5* (*ABI5*), *ABSCISIC ACID RESPONSIVE ELEMENTS-BINDING FACTOR 3* (*ABF3*), *G-BOX BINDING FACTOR 2* (*GBF2*), *GBF3*, *MYB DOMAIN PROTEIN 3* (*MYB3*), *ABA AND HYDROGEN PEROXIDE-ACTIVATED TF ARABIDOPSIS THALIANA ACTIVATING FACTOR1* (*ATAF1*) and *NAC-LIKE, ACTIVATED BY AP3/PI* (*NAP*), respectively, were amplified from genomic DNA using Taq Phusion polymerase (New England BioLabs, Ipswich, MA, USA) and primers described in Supporting Information Dataset S1. Obtained fragments were cloned in pGEM-t Easy (Promega), re-amplified with AttB-tailed primers and BP-cloned into pDONR207 (Invitrogen). *Promoter::GUS* binary vectors were generated by LR recombination of the promoter fragments into the destination vector pGWB3.

The *BRC1* oestradiol-inducible plasmid is described in González-Grandío *et al.* (2013). For the oestradiol-inducible constructs of *ABF3* and *ABI5*, the cDNAs were amplified from

TRANSPLANTA vectors (Coego *et al.*, 2014) and cloned into the pMDC7 vector (Curtis & Grossniklaus, 2003). For the *GUS* oestradiol-inducible construct, the *GUS* CDS was amplified from pGWB3 and LR-recombined into pAB117 (provided by Prof. Dr Rüdiger Simon, HHU Düsseldorf). For the *promoter::LUCIFERASE* (*LUC*) constructs, genomic fragments of 1031, 2636, 470, 1534, 1587, 2265 and 3376 bp of *BETA CAROTENOID HYDROXYLASE 2* (*BCH2*), *MITOGEN-ACTIVATED PROTEIN KINASE KINASE KINASE 18* (*MAPKKK18*), *AT5G05220* and *SENESCENCE ASSOCIATED GENE 20* (*SAG20*), respectively, comprising the BRC1 binding peaks, were amplified from genomic DNA using primers described in Dataset S1 and cloned into pGWB435 (Nakagawa *et al.*, 2007). The *HB53* promoter was domesticated to Phytobrick standard by PCR mutagenesis using primers described in Dataset S1 and cloned together with a *GUS-GGSG-linker-LUC* coding sequence, the *HB53* intron and a *NOPALINE SYNTHASE* (*NOS*) terminator (GB0037) into the pDGB3 omega vector by Golden Braid reactions (Vazquez-Vilar *et al.*, 2017).

Transient agroinfiltration assays and luminescence quantification

Agroinfiltration was performed as described (González-Grandío *et al.*, 2021). After 3 h of induction, three *Agrobacterium tumefaciens* cultures, each carrying one plasmid (*promoter::LUC* and two oestradiol-inducible plasmids), were resuspended in induction medium to optical density $(OD)_{600}$ of 0.1 and two *Nicotiana benthamiana* plants were infiltrated with different combinations (in a 1 : 1 : 1 ratio). An oestradiol-inducible *GUS* plasmid was included in combinations in which only oestradiol-inducible *BRC1*, *ABF3*, or *ABI5* were infiltrated. Three days after infiltration, four 6-mm leaf discs per leaf were incubated in 150 µl of MS in a 96-well white LUMITRAC 200 plate (Greiner Bio-One, Madrid, Spain). Afterwards, 50 µl of MS medium containing D-luciferin (Molecular Probes, Eugene, OR, USA) and oestradiol (Sigma-Aldrich) were added to a final concentration of 118 and 5 µM, respectively. Luminescence was measured using a Mithras LB 943 luminometer (Berthold, Bad Wildbad, Germany), measuring each well for 3 s every 10 min, for a period of 24 h. The maximum luminescence value for each leaf in this period was used.

Generation of transgenic plants

Binary vectors were transformed into the *A. tumefaciens* strain AGL-0. Transgenic Arabidopsis plants were generated by agroinfiltration using the floral dip method (Clough & Bent, 1998). At least 10 T3 homozygous lines were generated and analysed for each construct.

GUS staining

Flowering rosettes were dissected to expose the axillary buds. GUS stainings were performed as described (Sessions *et al.*, 1999). Samples were fixed 20 min in ice-cold 90% acetone and rinsed with water. They were then incubated with staining solution (100 mM Tris pH 7, 50 mM NaCl; 2 mM 4-cloro-3-indolil beta-D-glucuronic acid cycloheximide salt; 10 mM $K_3Fe(CN)_6$; 10 mM $K_4Fe(CN)_6$ $3H_2O$; Triton 0.2%) at 37°C for 16 h. After staining, samples were dehydrated in 30% ethanol in continuous light to remove the chlorophyll and rehydrated for analysis.

RNA-Seq and ChIP-Seq material collection

For the RNA-Seq experiment, plants of *brc1-2* (control) and *GFP::BRC1^{ind}* lines were grown on plates. Ten-day-old seedlings were induced with 5 ml of 10 µM oestradiol per plate. After an induction period of 5 h, 1 g of tissue was harvested for each of the three biological replicates. Total RNA was isolated using the InviTrap® Spin Plant RNA Mini Kit according to the manufacturer's protocol. TURBO™ DNase was used to clean the RNA samples from DNA. Library preparation for whole-genome RNA sequencing was done using the Illumina Truseq Library Preparation Kit. Library quality was evaluated using a Bioanalyzer and an RNA Nano 6000 kit (Agilent, Santa Clara, CA, USA). RNA concentrations were determined using the Xpose 'DSCVRY' (Trinean, Gent, Belgium). The libraries were then sequenced on the Illumina Hi-Seq 2500.

For the ChIP-Seq experiment, plants of *GFP::BRC1^{ind}* lines were grown on plates. Ten-day-old seedlings were induced with 5 ml of 10 µM oestradiol per plate. After an induction period of 5 h, 1.5 g of tissue was collected per sample. ChIP was performed as described (van Mourik *et al.*, 2015), using µMACS Anti-GFP beads (Miltenyi). Input DNA was used as control, which is isolated from the sonicated chromatin before immunoprecipitation.

Identification of genes co-regulated with *BRC1*-dependent genes

BRC1-dependent genes were obtained from González-Grandío *et al.* (2013). To investigate the function of these genes, we used the tools available in ATTED-II v.9.2 (http://atted.jp; Obayashi *et al.*, 2018) with the dataset Ath-m.c7-1 that comprises 14 668 publicly available microarray experiments (Obayashi *et al.*, 2018). We first used the tool HCLUSTER (with averaged linkage method) to cluster our target genes. This method computes an all-against-all distance matrix, quantifying the degree of co-expression between the target genes. The distance is obtained after a number of transformations of Pearson's correlation coefficients between co-expressed genes (see Obayashi *et al.*, 2018 for details). Next, this matrix was used to perform hierarchical agglomerative clustering with the averaged linkage method, until all genes were joined into a single cluster. Visual inspection of the clustering revealed six clusters immediately before all genes were joined within a single cluster, which were taken as a reference for further exploration.

To explore the biological significance and consistency of these clusters, we expanded the number of co-expressed genes by using the 'guilt by association' approach. Each gene cluster was independently input in CoEx-Search (ATTED-II; Obayashi *et al.*, 2007) to obtain a list of co-expressed genes. This preliminary expanded list contained 2700 genes for the six clusters. The

expression of these genes was finally validated considering the original arrays (with six biological replicates for each sample, González-Grandío *et al.*, 2013). Only genes up/downregulated (positive/negative fold change) in WT buds treated with white light supplemented with far-red light (WL + FR, dormant buds) but not in WT WL-treated or *brc1* mutant buds (active buds) were included in the final extended list of *BRC1*-dependent genes containing 947 genes. This list was subsequently cross-validated with independent ChIP-Seq and RNA-Seq experiments to identify the 97, final *bona fide* BRC1 direct target genes.

Functional annotation of *BRC1*-dependent clusters

Gene Ontology (GO) automated analyses of function prediction were carried out using a statistical overrepresentation test (*P*-value < 0.05) followed by Bonferroni correction for multiple testing in the PANTHER classification system (Mi *et al.*, 2017).

Differential gene expression and Gene Ontology enrichment analyses

Libraries of three biological replicates were sequenced individually and analysed using the BOWTIE–TOPHAT–CUFFDIFF (BTC) pipeline (Trapnell *et al.*, 2012). Differential gene expression was determined for all oestradiol-induced *GFP::BRC1*^{ind} samples, using oestradiol-induced *brc1-2* samples as control. The cut-off was set at a false discovery rate (FDR) < 0.05 in all analyses performed. The RNA-Seq data are made available via NCBI and can be accessed through GEO accession no. GSE155028. The BINGO v.3.03 plug-in (Maere *et al.*, 2005), implemented in CYTOSCAPE v.2.81 (Shannon *et al.*, 2003), was used to determine and visualise the GO-enrichment categorisation. A hypergeometric distribution statistical testing method was applied to determine the enriched genes in combination with the Benjamini and Hochberg multiple testing correction (FDR < 0.05).

ChIP-Seq data analysis

Libraries of three biological replicates of both the ChIP and Input samples were sequenced after which BOWTIE2 was used to map the reads to the Arabidopsis genome (Langmead & Salzberg, 2012). MACS2 was used for peak calling (Zhang *et al.*, 2008) using the Input samples as control. The ChIP-Seq data are made available via NCBI and can be accessed through GEO accession no. GSE155028. The function Distance2Genes, part of the R-package CSAR, was used to determine the nearest gene (Muiño *et al.*, 2011). These nearest genes are then presented in a list of candidate target genes (van Mourik *et al.*, 2015) for further analysis. The analysis of read distribution of our ChIP-Seq dataset was done by the R-package CHIPPEAKANNO: 'assignChromosomeRegion'. As a cut-off 1 kb of promoter region with an immediate cut-off of 0.5 kb was used. To assess the reproducibility of the datasets, a pairwise correlation analysis was done on the relative enrichment values of the peaks in the list of candidate target genes, and a principal component analysis (PCA) based on counts per genomic bin of the three samples and their input. For the datasets of the first two repetitions, a file was created representing their overlap, which was inferred by the distance between peaks in the individual samples. The average peak size was ±300 bp, so if the centre of a peak in one sample is no more than 150 bp apart from the centre of a peak in the other sample, the peaks are assumed to be in fact the same and were saved in a separate file for subsequent analyses. This criterion resulted in a file containing roughly 60–70% of the peaks of samples 1 and 2. Since this merging of peaks may result in a slight shift of the actual binding site, analyses looking specifically at the exact location of the binding site were done on the individual samples 1 and 2 datasets.

Analysis of peak-overlap between BRC1 and BTFs

We use as datasets the 4227 BRC1 peak locations and the peak locations and target genes for nine BTFs. We defined promoter regions as 3-kb upstream region according to TAIR. For each BTFs, we performed the following analysis: We obtained the promoter region of the BTF target genes; retrieved the peak locations of BTF occurring in those promoter regions (at least 1 bp of the peak should be in the promoter region); obtained the peak locations of BRC1 occurring in those promoter regions, for each BRC1 peak occurring in those promoter regions, and checked whether there is a BTF overlapping peak (defined as having at least 1 bp in common). To infer the significance of the observed overlap, we tested the null hypothesis that the position of BRC1 peaks and BTF peaks occurring in the same promoter was independent of each other, using 1000 reshuffled versions of the peak lists. Reshuffling was performed by picking, for each peak independently, a random position in the promoter region (hence changing the position but not the promoter region in which the peak occurred). The *P*-value in this test was obtained as the fraction of reshufflings (out of 1000), which resulted in a number of overlapping peaks higher than the actual observed number of overlapping BRC1-BTF peaks.

Motif enrichment analysis

Motif discovery was carried out using MEME, DREME and CentriMO of the MEME-CHIP programme (Machanick & Bailey, 2011). MEME (Bailey & Elkan, 1994) looks for overrepresented motifs in a set of sequences compared with a background model of nucleotide frequencies. The background model was generated using fasta-get-markov for the MEME suite, using a second-order Markov model, and a set of 207 randomly selected sequences from Arabidopsis promoters as input. DREME (Bailey, 2011) looks for motifs occurring significantly more often in the input set of sequences compared with a control set; as control set, shuffled versions of the input set was used. CentriMO (Bailey & MacHanick, 2012) is used to test whether the motifs found are centrally enriched. In the present study, motifs were investigated to detemine whether they were in the top six motifs as defined by MEME-CHIP. Default settings for DREME were used, including an *E*-value threshold of 0.05. Default settings for MEME were used, with the following exceptions: the setting

meme-mod-anr was used, which assumes zero, one or multiple motif occurrences per sequence. Minimum and maximum width for the motifs was set to 4- and 15 bp, respectively.

Network construction and visualisation

The transcriptional network comprising the *BRC1*-dependent genes and the potential targets of the *BRC1*-dependent TFs was constructed using the R package IGRAPH for network construction and analysis and ChIP-Seq and DNA Affinity Purification and sequencing (DAP-Seq) data available (O'Malley *et al.*, 2016; Song *et al.*, 2016). Nodes represent genes, and directed edges were drawn from $gene_i$ to $gene_j$ when $gene_i$ encodes a TF that binds to the promoter of $gene_j$. A binary directed network adjacency matrix of size 947 × 947 (all-against-all genes) was constructed by setting component (i, j) to 1 when $gene_i$ encodes a TF that binds to $gene_j$ promoter, and it was set to 0 otherwise. The function *graph.adjacency* with input the previously described adjacency matrix and argument *mode* equal to *directed* was used to generate our network comprising 947 nodes/genes and 10 240 edges/potential direct transcriptional regulations. A web app was developed using the R package SHINY to analyse this network, available at the URL https://greennetwork.us.es/BRC1NET.

Network motif identification and analysis

A network motif is defined as a subgraph whose occurrence is significantly greater in our network than its occurrence in random networks (Milo *et al.*, 2002; Alon, 2007). The analysis was performed using the R package IGRAPH. The network has 947 nodes, 37 of them representing TFs in BRC1NET for which ChIP-Seq or DAP-Seq data are available (regulatory set) and the remainder 910 nodes representing their regulated target genes. Elements of the regulatory set can also be regulated by other members of the set or by themselves. Therefore, nodes in the regulatory set are the only ones having output edges but they may also have input edges, while the regulated set only has input edges. We considered two randomisations with an increasing degree of stringency in preserving the constraints observed in the real network. In both randomisations, 10 000 random networks were generated with the same number of nodes, edges and out-degree. In the first randomisation, the targets of the regulatory set were randomly selected among all nodes (including the regulatory set itself). Therefore, the in-degree of the nodes was not conserved. The intended purpose of this randomisation is to test whether regulation within the regulatory set is significantly higher than expected by chance and, if it is, what are the most significant motifs. In the second randomisation, the in- and out-degree of all nodes in the network were conserved exactly. The purpose of this second randomisation is to test what motifs found in the first randomisation remain significant if the proportion of links within the regulatory set and their degrees are fixed, hence highlighting their importance in regulation. This randomisation was implemented following an extension of the curveball algorithm for directed networks (Carstens *et al.*, 2018). We verified that 10^5 steps of the algorithm were sufficient to ensure an unbiased search. The R source code for this algorithm and the rest of scripts used for the construction and analysis of BRC1NET are available in the GitHub repository https://github.com/fran-romero-campero/BRC1NET to ensure reproducibility of our results.

Results

BRC1 regulates nine co-expression gene clusters

To identify the genes regulated by *BRC1*, we first performed an *in silico* reanalysis of available expression data. González-Grandío *et al.* (2013) carried out a transcriptional profiling of WT and *brc1* mutant axillary buds of plants exposed to 8 h of white light enriched in far-red light (WL + FR), simulating a canopy shade. In WT (but not in *brc1* mutants), this leads to *BRC1* mRNA accumulation and bud dormancy. We used the collection of genes differentially expressed (DE) (FDR < 0.05) in response to *BRC1* (*BRC1*-dependent genes, Fig. S1) as a starting point for this study. To investigate their potential functional relationships, we studied their degree of co-expression in > 14 668 publicly available microarray experiments and clustered them by their global similarity of transcriptional responses (see the Materials and Methods section). This analysis revealed six co-expression clusters of upregulated genes and three co-expression clusters of downregulated genes (Fig. 1a). We searched *in silico* for additional genes co-expressed with members of each cluster and retained only those that were *BRC1*-dependent, that is, they were DE in dormant (WL + FR-treated WT) buds, but not in active (WL-treated WT, or *brc1* mutant) buds (Fig. 1b). These genes were added to the *BRC1*-dependent category (Figs S1, S2). We termed the clusters of co-expressed genes, UP_C1 to C6 and DOWN_C1 to C3, for the up- and downregulated genes in dormant buds, respectively (Fig. 1b; Dataset S2).

Each co-expression cluster was enriched in a different set of GO terms (Mi *et al.*, 2017; Fig. 1a; Dataset S2): UP_C1 was enriched in genes involved in ethylene signalling, senescence and catabolism; UP_C2, in genes related to water transport; UP_C3, brassinosteroid and auxin signalling; UP_C4, response to light; UP_C5 did not show an statistically significant enrichment in GO terms, but contained genes related to cell wall remodelling and GA signalling, among others; UP_C6 was enriched in genes related to ABA signalling and response to abiotic stress; DOWN_C1, genes related to chloroplast activity and organisation; DOWN_C2, DNA replication and cell division; and DOWN_C3 genes related to biosynthesis of secondary metabolites such as flavonoids, glucosinolates and pectins.

This collection of 947 genes (Dataset S2) constitutes a core transcriptional response associated with *BRC1* activity and to the growth-to-dormancy transition in Arabidopsis axillary buds.

Identification of BRC1 direct targets

We next investigated how BRC1 orchestrated the expression of these *BRC1*-dependent gene clusters in buds. BRC1 could directly regulate the expression of a majority of genes from each cluster, or could control a limited number of key regulators,

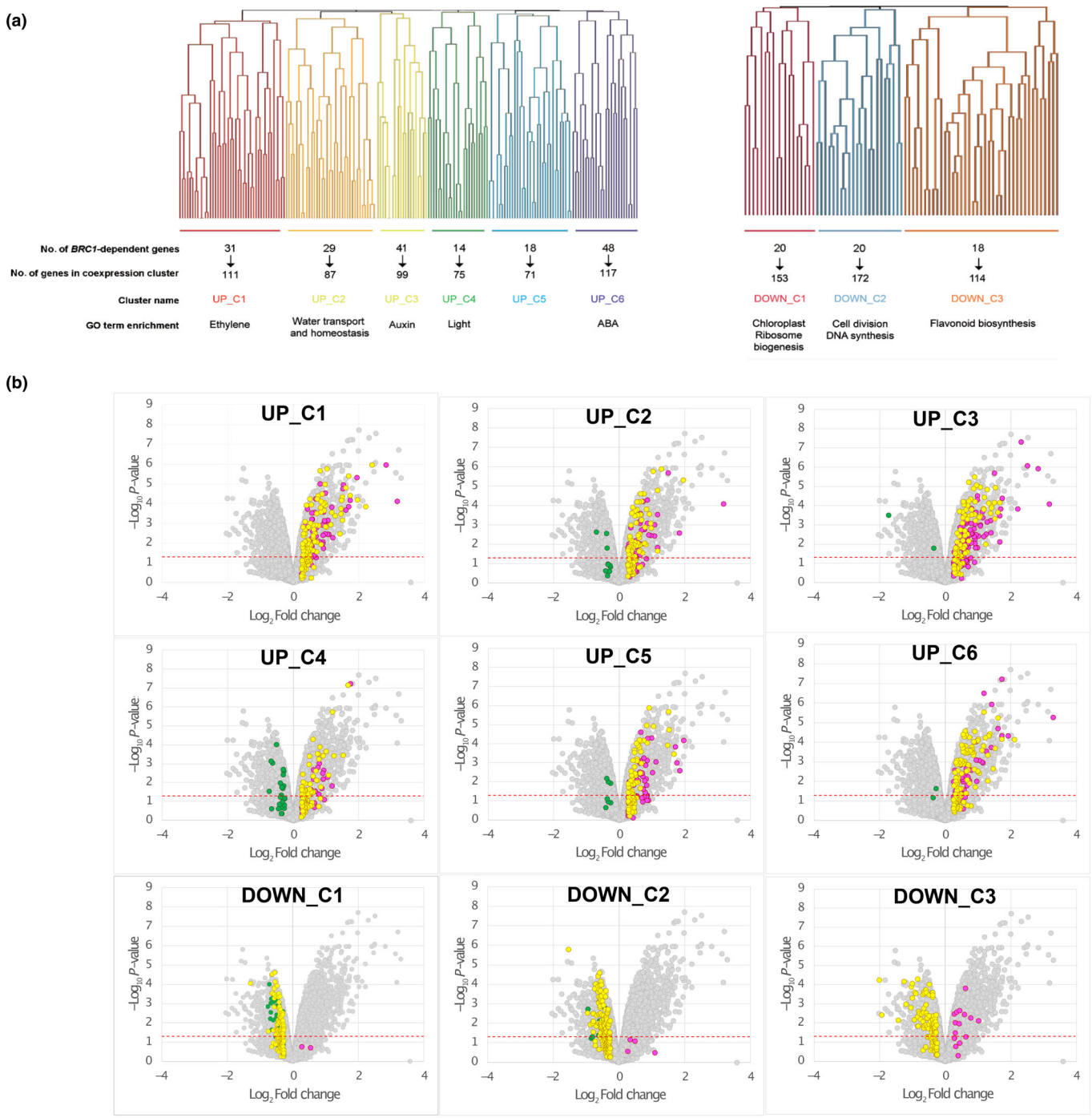

Fig. 1 *BRANCHED1* (*BRC1*)-dependent gene co-expression clusters. (a) Hierarchical clustering of *Arabidopsis thaliana BRC1*-dependent genes (González-Grandío *et al*., 2013) based on their degree of co-regulation in 14 668 microarray experiments (ATTED-II, Obayashi *et al*., 2018). Only 238 (181 UP and 57 DOWN) of the 307 genes are represented in Affymetrix arrays and could be analysed. Number of co-regulated genes, number of additional co-expressed genes, cluster name and representative overrepresented Gene Ontology (GO) terms are indicated for each cluster. (b) Validation of genes co-expressed with *BRC1*-dependent genes. Volcano plots representing *P*-value ($-\text{Log}_{10}$ *P*-value, vertical axis) and relative expression (Log_2 fold change, horizontal axis) of genes in the active vs dormant buds (8 h low R : FR vs High R : FR) transcriptome. *BRC1*-dependent genes and their co-expressed genes are highlighted. Yellow dots represent the original *BRC1*-dependent genes plus those co-expressed genes induced or repressed only in wild-type (WT) but not in *brc1* mutants. These genes were further analysed. Magenta dots represent genes induced both in WT and *brc1* mutant buds. Green dots, genes repressed both in WT and *brc1* mutant buds. Genes with green and magenta dots were not included in subsequent analyses.

which in turn mediate a wider transcriptional response. To discern between these possibilities, we looked for direct BRC1 targets in the Arabidopsis genome using ChIP-Seq (Kaufmann *et al*., 2010). *BRC1* expression levels are low and limited to axillary buds (Aguilar-Martínez *et al*., 2007), which complicate the study of protein-DNA-binding events (Kidder *et al*., 2011). We

therefore performed ChIP in 10-d-old seedlings of oestradiol-inducible lines *LEXA::GFP::BRC1*^{ind}; *brc1-2* (*BRC1*^{ind}) (González-Grandío *et al.*, 2017). We collected material 5 h after beginning of the oestradiol induction, when the GFP::BRC1 protein accumulated at high levels (González-Grandío *et al.*, 2017) and performed ChIP-Seq for three independent biological replicates (Fig. S3; Dataset S3). This experiment resulted in the identification of 4339 loci that contained BRC1 peaks within 3-kb upstream of the TSS. A large proportion (*c.* 60%) of the BRC1 peaks were located in the proximal upstream region of protein-coding genes, predominantly within 300 bp of the transcription start site (TSS) (Fig. 2a). Because of the lower number of peaks in sample 3 (Figs 2a, S3a) a pairwise correlation analysis was performed for the relative enrichment values of the peaks in the list of candidate target genes, revealing Pearson correlation coefficients ranging from 0.77 to 0.83 (Fig. S3b). Additionally, a PCA analysis was done, which separated sample 3 from the other two samples (Fig. S3c). Based on these observations, we decided to perform further analyses on samples 1 and 2.

About 4000 loci (*c.* 60%) contained peaks within 3-kb upstream of their TSS whereas the other peaks were positioned in introns, exons or UTRs (total *c.* 9%), and the remaining *c.* 10 and *c.* 20% in the downstream and intergenic regions, respectively (Fig. 2b). This distribution was comparable to that found for ChIP-Seq performed on other Arabidopsis TFs (e.g. Kaufmann *et al.*, 2009; Bencivenga *et al.*, 2016), but divergent from that described for cucumber TEN, a closely related TCP factor, for which a large proportion of binding sites are localised in gene bodies (Yang *et al.*, 2020).

BRC1-bound peaks in the two most enriched ChIP-Seq samples showed a significant overrepresentation of several motifs (Table S1, DREME; Bailey, 2011), most notably GDCCCA and BACGTGKC (D = AGT; B = CGT; K = GT) (Fig. 2c). About 60% (57.5% and 65.1% for samples 1 and 2, respectively) of all peaks contained the GDCCCA motif, which closely resembles a TCP-binding site (González-Grandío & Cubas, 2015; O'Malley *et al.*, 2016) and the BRC1-binding motif GGgcCCmc, inferred by protein-binding microarray assays (González-Grandío *et al.*, 2017). Remarkably, 50% of all peaks (48.3% and 51.9% for samples 1 and 2, respectively) contained the BACGTGKC motif, which closely resembles a G-box (CACGTG) recognised by bHLH and bZIP TFs (Menkens *et al.*, 1995). Interestingly, in *c.* 30% of the peaks (28.5% and 34.5% for samples 1 and 2, respectively), the TCP-binding site was accompanied by a G-box-like motif. In these cases, the TCP motif was centrally enriched, whereas the G-box was positioned either up- or downstream of the TCP-binding site (Fig. 2d). This suggests that BRC1 frequently acts in concert with G-box-binding proteins to control gene expression. The overrepresentation of a G-box-like motif was not reported in the recently published ChIP-Seq experiment for maize TB1 (Dong *et al.*, 2019), and this prompted us to reanalyse that dataset. Our analysis confirmed that the G-box is also overrepresented in the maize TB1 targets (Notes S1), revealing that this feature is indeed conserved in maize, a monocot distantly related to Arabidopsis.

In parallel to the ChIP-Seq study, we did a gene expression analysis (RNA-Seq) in Arabidopsis of similar oestradiol-treated material, to identify genes responding to *BRC1* activity (DE genes, DEG; Dataset S4). We found 5718 DEGs of which 1845 were upregulated and 3873 were downregulated after induction (FDR < 0.05). We considered *BRC1 direct targets* those genes whose regulatory regions were bound by BRC1 (i.e. *BRC1-bound genes*) and were DE after *BRC1* induction in seedlings (Fig. S1). We identified 1438 BRC1 direct targets according to this criterion.

BRC1-dependent direct gene targets

To further refine the BRC1 target gene list, we compared the BRC1 direct targets identified by ChIP-Seq and RNA-Seq in seedlings with the nine clusters of *BRC1*-dependent genes identified in the axillary bud transcriptomics. Genes present in the three lists were considered *bona fide* BRC1 direct target genes (Fig. S1; Dataset S5). We identified 97 *bona fide* BRC1 direct target genes, 90 induced and seven repressed in response to *BRC1* both in seedlings and in buds entering dormancy. This strongly indicates that BRC1 acts mainly as a transcriptional activator. Moreover, we confirmed that the ChIP-Seq and RNA-Seq data obtained from seedlings had biological significance, as the *BRC1*-dependent UP clusters obtained in buds (especially UP_C4 and UP_C6) were very significantly enriched in BRC1-bound, DEG and BRC1 direct targets identified in seedlings (Fig. S4a,b,d). By contrast, the DOWN clusters were not enriched in these gene lists, further supporting the role of BRC1 as a transcriptional activator (Fig. S4a,c,e).

The *bona fide* gene list (Dataset S5) was enriched in genes containing ABA-related terms (ABA signalling, FDR = 0.045; ABA response, FDR = 7.4×10^{-4}; ABA transport, FDR = 0.037) and genes responding to water deprivation and salt/osmotic stress (FDR = 0.01). Another significantly enriched category (FDR = 0.037) was regulation of transcription: 19 *bona fide* BRC1 direct targets encoded TFs, many of which had ABA-related annotations. The list also contained induced genes encoding enzymes controlling hormone metabolism and homeostasis such as *MORE AXILLARY BRANCHES1* (*MAX1*), *NINE-CIS-EPOXYCAROTENOID DIOXYGENASE 3* (*NCED3*) and *CYTOSOLIC SULFOTRANSFERASE 15* (regulating SL, ABA and JA synthesis respectively, Gidda *et al.*, 2003; Ruggiero *et al.*, 2004; Booker *et al.*, 2005); *BCH2* that catalyses the synthesis of zeaxanthin, a precursor of SL and ABA; *ABSCISIC ACID 8′-HYDROXYLASE 2*; and *GA 2-BETA-DIOXYGENASE 2* (*GA2OX2*) (involved in ABA and GA degradation respectively); and *INDOLE-3-ACETIC ACID-AMIDO SYNTHETASE GH3.5* (that control auxin amino acid conjugation). Among the six downregulated genes was *UDP-GLYCOSYLTRANSFERASE 76C2* (that promotes cytokinin glycosylation and inactivation). Induced direct targets of BRC1 were also genes encoding ubiquitination-related proteins. Finally, BRC1 directly regulates genes encoding transmembrane proteins involved in inter- and intracellular transport of water and reactive oxygen species (the aquaporins *PLASMA MEMBRANE INTRINSIC PROTEIN (PIP)1B/PIP1-2*, *PIP1C/PIP1-3*, *PIP2E/PIP2-6*), ions

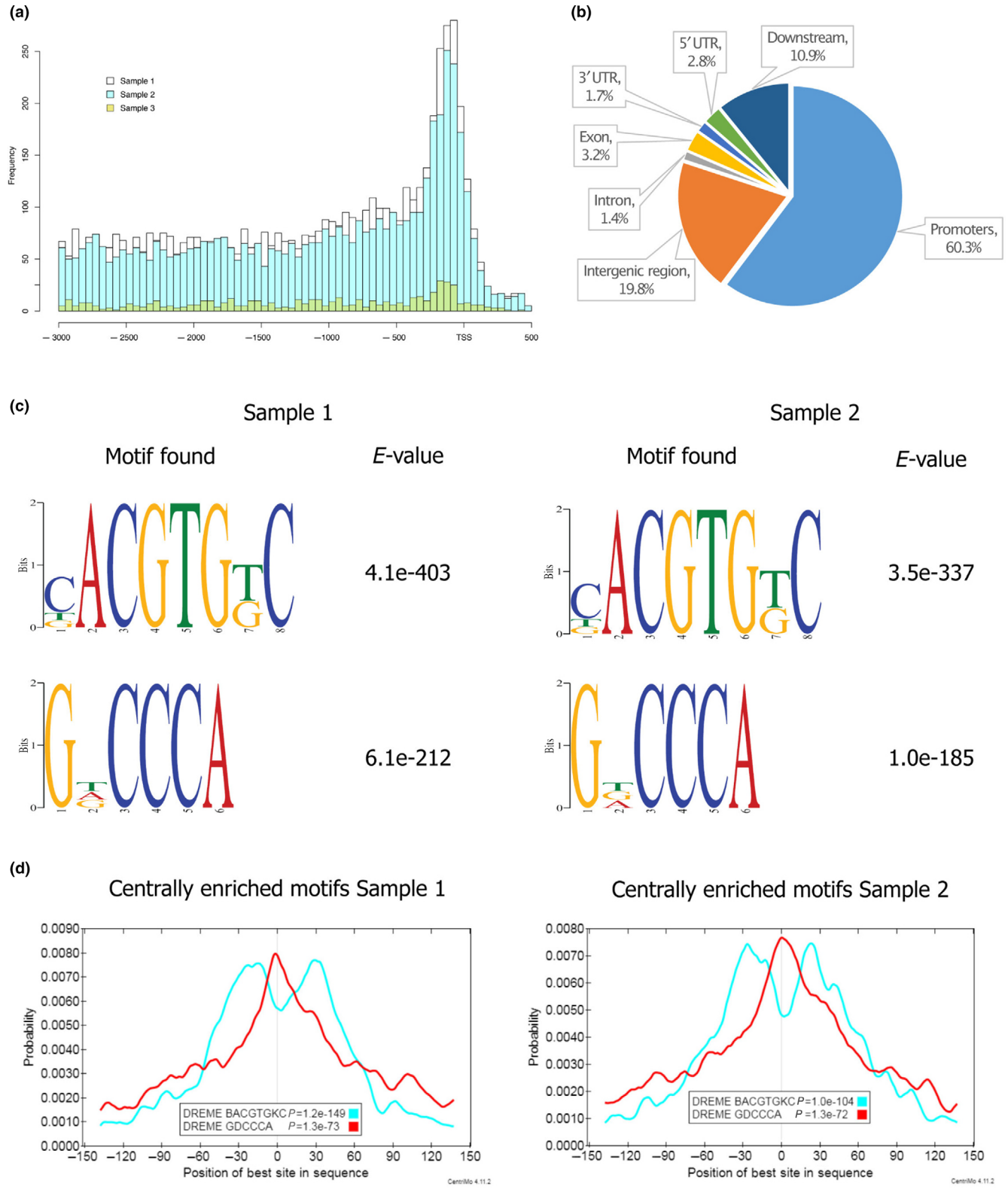

Fig. 2 Overview of chromatin immunoprecipitation sequencing (ChIP-Seq) data and MEME motif enrichment analysis. (a) Sequencing read distribution 3-kb up- to 500-bp downstream of the transcription start site (TSS) in *Arabidopsis thaliana* BRANCHED1 (BRC1)-bound loci. (b) Distribution of reads over the different regions in the identified BRC1-bound loci (promoter, intron, exon etc). (c) Results of the MEME motif enrichment analysis. Specific enrichment was found for a consensus BRC1 TEOSINTE BRANCHED1, CYCLOIDEA, PCF (TCP)-like binding motif and a G-box motif. (d) Localisation of the identified motifs in the BRC1-bound regions. The GDCCCA (motif 2; TCP-binding motif) is centrally enriched, whereas the CACGTG (motif 1; G-box) is found enriched in short distance up- or downstream of the ChIP peak centre.

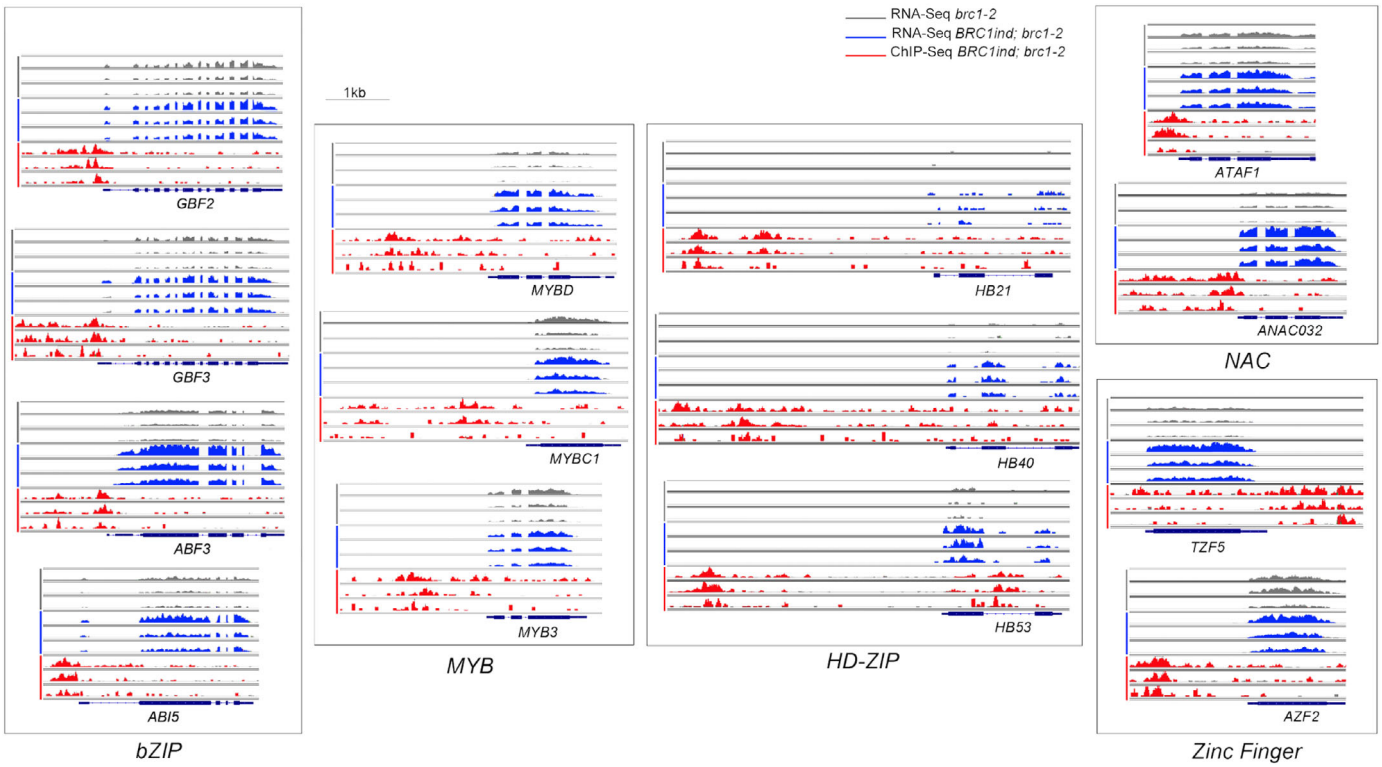

Fig. 3 Transcription factors directly regulated by *Arabidopsis thaliana* BRANCHED1 (BRC1). BRC1 binding peaks (red) and *BRC1*-induced differential gene expression (blue) for 12 genes encoding BRC1-regulated transcription factors (BTFs) of the bZIP, NAC, MYB and Zinc Finger families. *MYB3* and *AZF2* (*BRC1*-dependent and BRC1-bound but not differentially expressed in seedlings) are also included as potential additional BRC1 targets in buds.

(*AT1G69480*, *AT1G79520*, *AT5G17850*, *AT1G58340*, *AT4G27280*, *AT3G56290* and *NRT1:2*), glycerol-3-phosphate (*AT4G17550*) and ABA (*ARABIDOPSIS THALIANA ATP-BINDING CASSETTE G25*, *ATABCG25*; *NRT1:2*) as well as other transmembrane proteins of yet unclear function (*AT2G47770*, *AT3G13720*, *AT1G27670*, *AT3G57400*, *AT3G45600* and *AT5G64260*).

All these results indicate that BRC1 directly controls the expression of numerous genes related to ABA function, and the activity and homeostasis of other hormones involved in bud activity such as SL, GA, auxin and cytokinin (Barbier *et al.*, 2019), as well as JA, which promotes defence against abiotic and biotic challenges and effectively represses cell division (Świątek *et al.*, 2002). BRC1 may also modulate the intra- and intercellular transport of nutrients, signals and water in the cells of axillary buds. Finally, BRC1 regulates a remarkable collection of TFs, which may play a relevant role in the control the BRC1 transcriptional network.

Some BRC1 direct target genes encode TFs that bind G-box motifs

Bona fide BRC1 direct targets were enriched in genes encoding TFs that we termed *BRC1-targeted TFs* (BTFs): HD-Zip genes *HB21*, *HB40* and *HB53*; bZIP genes *GBF2*, *GBF3*, *ABF3* and *ABI5*; NAC genes *ATAF1* and *NAC032*; AP2/EREB genes *ERF113/Rap2.6L* and *CRF6*; MYB genes *MYBC1*, and *MYBD*; zinc finger protein gene *ATTZF5*; and heat shock protein gene *HSB2A* (Fig. 3; Table 1).

Several of these BTFs (i.e. GBF2, GBF3, ABF3, ABI5, ANAC032 and ATAF1) bind G-box-like motifs, in which BRC1 peaks are enriched (as mentioned above), and GBF2 and GBF3 also bind TCP-like motifs after ABA treatments (Fig. S5). This raises the possibility that BTFs act as co-regulators of the *BRC1*-dependent network together with BRC1. Consistently, *in silico* analyses in search for regulators of the *BRC1* network (TF2Network tool, Kulkarni *et al.*, 2018; Plant Regulomics, Ran *et al.*, 2020) also predicted some of these BTFs as potential regulators of the network (i.e. ABI5, GBF2, GBF3, ABF3, ATAF1, MYBD, HB21, HB40, HB53; Dataset S6).

To investigate whether the BTFs preferentially targeted the *BRC1*-dependent genes, we studied their genome-wide binding sites using publicly available ChIP-Seq and DAP-Seq data (O'Malley *et al.*, 2016; Song *et al.*, 2016). Remarkably, the BTF targets were significantly enriched in *BRC1*-dependent BRC1-bound and *bona fide* BRC1 targets (Fig. 4a). Fine mapping of binding peaks revealed that, in genes bound both by BRC1 and a BTF, a large proportion of the BRC1 peaks co-occur with BTF peaks (Fig. 4b). This suggests that BTFs act in close cooperation with BRC1 to control transcription (Fig. 5a). Furthermore, not one but several BTF peaks usually overlap with BRC1 peaks at the promoters of BRC1 *bona fide* gene targets (Fig. 5b,c). In the *BRC1*-dependent gene targets not bound by BRC1, the peaks of the different BTFs also overlap (Fig. 5d).

Table 1 BRC1-regulated transcription factors (BTFs).

AGI name	Name	Description	TF family
At4g36740	**ATHB-40**	**Homeobox-leucine zipper protein ATHB-40**	**HD-zip**
At5g66700	**ATHB-53**	**Homeobox-leucine zipper protein ATHB-53**	**HD-zip**
At2g18550	**ATHB-21**	**Homeobox-leucine zipper protein ATHB-21**	**HD-zip**
At4g01120	**GBF2**	**G-box-binding factor 2**	**bZIP**
At2g46270	**GBF3**	**G-box-binding factor 3**	**bZIP**
At4g34000	**ABF3**	**ABA-responsive element-binding factor 3**	**bZIP**
At2g36270	**ABI5**	**ABA-insensitive 5**	**bZIP**
At1g77450	**ANAC32**	**NAC domain-containing protein 32**	**NAC**
At1g01720	**ATAF1/ ANAC002**	**ATAF1/ANAC domain-containing protein 2**	**NAC**
At1g70000	**MYBD**	**MYB-like transcription factor**	**MYB**
At2g40970	MYBC1	Homeodomain-like superfamily protein	Homeodomain
At5g13330	**ERF113/ Rap2.6 L**	**Ethylene-responsive transcription factor ERF113**	**ERF/AP2**
At3g61630	CRF6	Ethylene-responsive transcription factor CRF6	ERF/AP2
At5g49700	AHL17	AT-hook motif nuclear-localised protein 17	AT-hook
At5g44260	**TZF5**	**Tandem CCCH Zinc Finger protein 5**	**CCCH Zinc Finger**
AT5G62020	HSFB2A/ HSF6	Heat stress transcription factor B-2A	HSF
At1g19050	ARR7	Response regulator 7	ARR
At4g31800	**WRKY18**	**WRKY transcription factor 18**	**WRKY**
At1g07090	**LSH6**	**Light-dependent short hypocotyl 6**	**ALOG**

List of *Arabidopsis thaliana* BRC1 direct targets encoding TFs. In bold, those related to ABA signaling and/or response.

The BRC1 transcriptional network is enriched in multi-output feed-forward and regulated feedback loops

To further explore the regulatory interactions between BRC1, BTFs and other TFs, we constructed and analysed a transcriptional network by integrating our BRC1 ChIP-Seq data with ChIP- and DAP-Seq data publicly available for 10 BTFs and 27 additional *BRC1*-dependent TFs (O'Malley *et al.*, 2016; Song *et al.*, 2016). The network comprises the 947 *BRC1*-dependent genes (Dataset S1). This transcriptional network, BRC1NET, can be accessed and analysed using an interactive web application available at https://greennetwork.us.es/BRC1NET. The BRC1NET application allows dynamic visualisation of specific and common targets for any TF or combination of TFs in the network. It generates target gene lists, performs significance and functional enrichment analyses, and allows visualisation of TFs binding peaks and binding motifs in any given gene of the network (Fig. S6).

Using the BRC1NET enrichment analysis tool, we discovered that some BTFs could be preferentially regulating specific *BRC1*-dependent clusters. For instance, GBF2, GBF3, ABF3 and ANAC032 were identified as potential regulators of the ethylene-related cluster UP_C1. Similarly, ABF3, ABI5 and ANAC032 are potential regulators of the ABA-related cluster UP_C6. None of the DOWN clusters was significantly targeted by any BTF (Tables S2, S3; Fig. S7).

Next, we performed a network motif enrichment analysis of BRC1NET, using two different null models with increasing stringency in preserving the constraints observed in the real network (see the Materials and Methods section), to identify non-random gene modules formed by TFs that co-ordinately orchestrate the regulation of common target gene sets (Dataset S7). With the first null model, which preserves the observed out-degrees, we found that this network has more regulation within the *BRC1*-dependent TFs than expected by chance. Notably, we found that this network is enriched in motifs such as multi-output FFLs and regulated multi-output FBLs, among others (Figs 5a, S8; Alon, 2007). Importantly, regulated FBLs were significantly enriched, even when a second and more stringent null model that preserved the in- and out-degrees of the network was considered (Fig. S8).

In multi-output FFLs, a master regulator TF1 binds the promoter of a gene encoding an intermediary regulator TF2. Both TFs bind the promoters of a common target gene set, thus regulating their expression (Figs 5a, S8d). In BRC1NET, a large number of FFLs comprise BRC1 and a BTF (i.e. ABI5, ANAC032, ATAF1, HB21, HB40, HB53 and GBF2) as TF1 and TF2 respectively. BRC1 and the BTF in turn regulate common target gene sets (Fig. 5a,b).

The BTFs are also involved in BRC1-regulated FBLs with multiple outputs: two BTFs (TF1 and TF2), regulate each other, and jointly control a set of common target genes (Figs 5a–c, S8b, c). The targets of these FBLs are not randomly distributed over the network. Rather, pairs of BTFs involved in FBLs, significantly regulate specific clusters (Tables S4, S5). For instance, the ABI5/ANAC032 FBL target gene set is significantly enriched (*P*-value 5.7×10^{-12}) in genes of the ABA-related cluster UP_C6 (Fig. S9), whereas the ABI5/ATAF1 FBL target gene set regulates cluster UP_C2 (*P*-value 5.3×10^{-5}). Interestingly, no FFLs or FBLs were identified that significantly regulate the DOWN clusters, which supports the position of these clusters downstream of but far away from the direct response triggered by BRC1.

This intricate *BRC1*-dependent network is highly redundant: a significant proportion of the 947 *BRC1*-dependent genes are targets of more than one BTF (e.g. Fig. 5b,c), which may render the GRN extremely robust to random mutations. Indeed, the predicted network connectivity is only mildly affected even after *in silico* removal of up to 10 TFs of the network (excluding BRC1, Fig. S10), which implies that a plant carrying mutations in all 10 of these TFs will likely still have a WT branching phenotype under standard conditions (to be described later).

All these results indicate that BRC1 regulates its GRN both directly, by forming FFLs and regulated FBLs with the BTFs (Fig. 5a–c), and indirectly, via numerous FBLs established among the BTFs and other *BRC1*-dependent genes not bound by BRC1 (Fig. 5a,d).

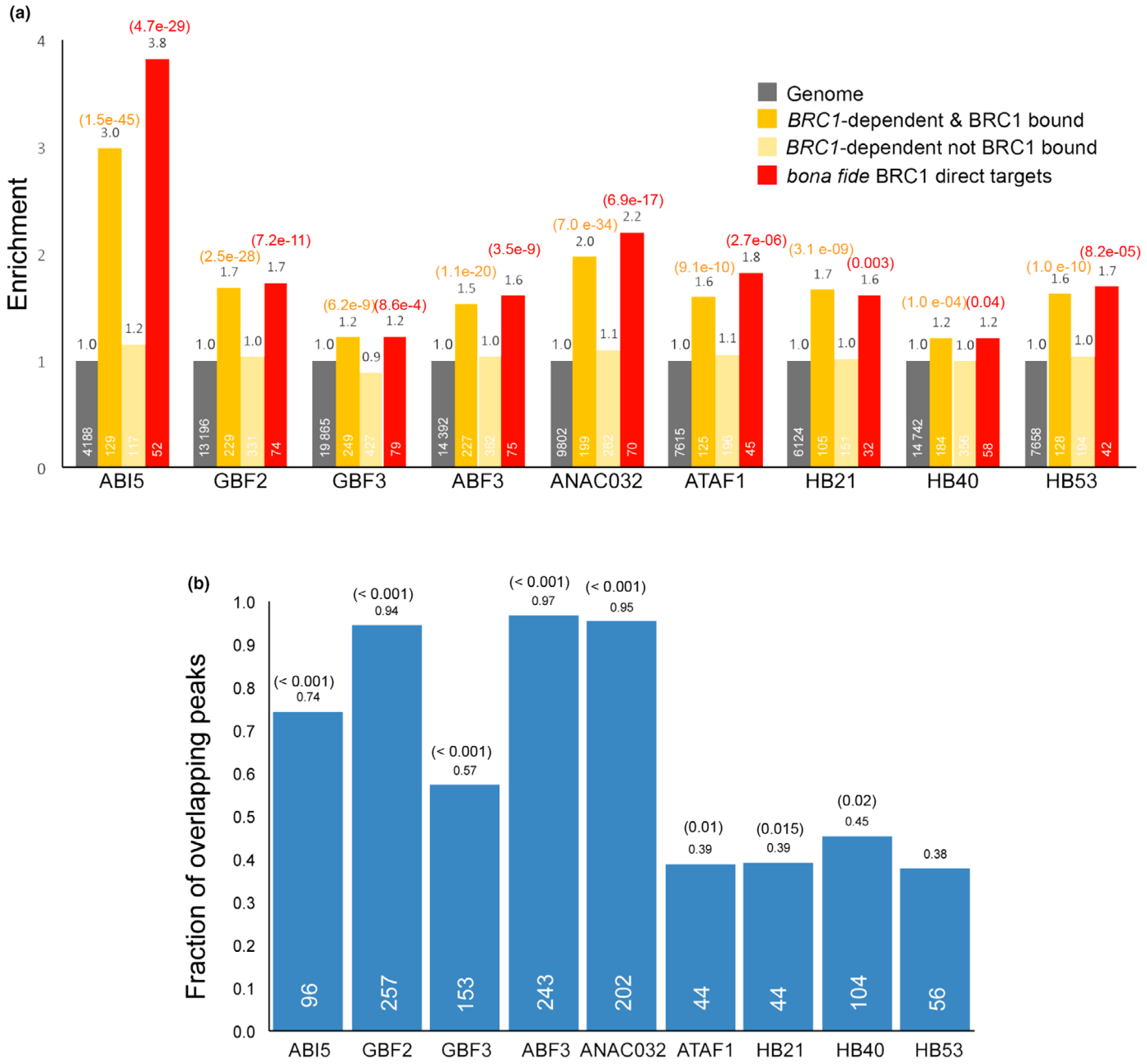

Fig. 4 BRANCHED1 (BRC1) and BRC1 targeted transcription factor (BTF)-binding sites largely overlap. (a) Enrichment of BTF gene targets in the following *Arabidopsis thaliana* gene sets: *BRC1*-dependent and BRC1-bound, *BRC1*-dependent not BRC1-bound and *bona fide* BRC1 direct targets. Numbers inside the bar indicate number of genes in each category. In parenthesis, *P*-values for significant (< 0.05) enrichments obtained from Pearson's chi-squared test with Yates' continuity correction. (b) Fraction of BRC1 peaks found in BTF target gene promoters, which overlap with BTF peaks. Number inside bar indicates number of BRC1 peaks occurring in promoters of BTF target genes that overlap with BTF peaks. In parenthesis, *P*-values for significant (< 0.05) overlap.

The BTFs are expressed in axillary buds

To validate the biological significance of our findings *in planta*, we first fused the promoters of some of these BTFs (*ABI5*, *ABF3*, *GBF2*, *GBF3* and *ATAF1*) to the reporter *β-GLUCURONIDASE* and transformed them into Arabidopsis. The resulting lines displayed, like *BRC1* (Aguilar-Martínez *et al.*, 2007), a strong *GUS* expression localised in axillary buds (Fig. 6a–i). *HB21*, *HB40* and *HB53* are also expressed in these structures (González-Grandío *et al.*, 2017). Furthermore, other *BRC1*-dependent, BRC1-bound genes encoding TFs (e.g. *NAP*, *MYB3*) were also highly and specifically expressed in axillary buds (Fig. 6j–l).

The BTFs modulate the transcriptional activity of BRC1

To further investigate the *in vivo* responses of this GRN, we tested some of the FFL identified. For that, we selected eight *bona fide* BRC1 direct targets (*HB53*, *BCH2*, *MAPKKK18*, *AT5G05220*, *SAG20*, *ABI5*, *ATAF1* and *GBF3*) whose promoters contained BRC1binding sites overlapping with those of two

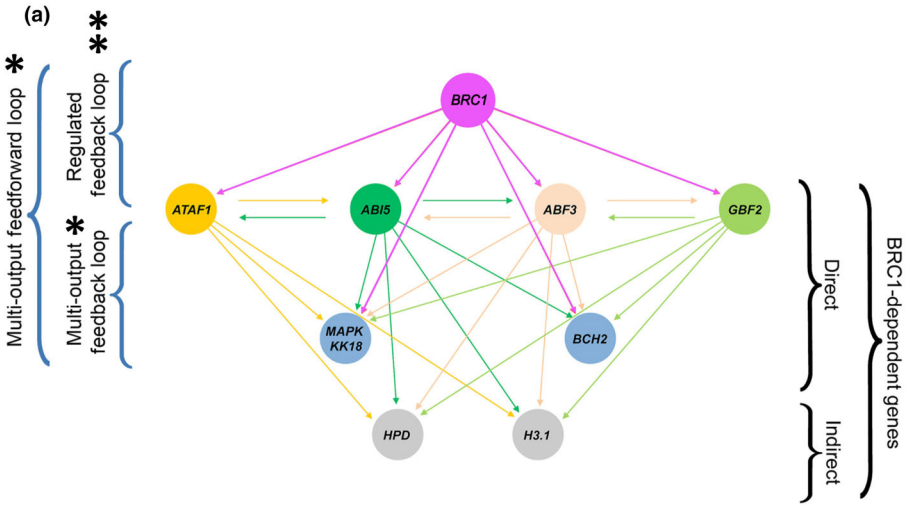

Fig. 5 Motifs overrepresented in the *Arabidopsis thaliana* BRANCHED1 (BRC1) network. (a) Simplified representation of the BRC1 network, that exemplifies overrepresented motifs (multi-output feed-forward loops (FFLs), regulated feedback loops (FBLs) and multi-ouput FBLs) using specific cases. Significance: *, < 1e-3 in null model 1; **, < 1e-3 in null models 1 and 2. Orange and green circles represent genes encoding BRC1 target genes encoding transcription factors (BTFs) (*ATAF1*, *ABI5*, *ABF3* and *GBF2*); blue circles, other *bona fide* BRC1 targets; grey circles, *BRC1*-dependent genes bound by BTFs but not by BRC1. Green and orange arrows indicate direct binding of the BTFs; magenta arrows, direct binding of BRC1. (b) Genomic region of genes encoding BTFs. The overlapping binding sites of BRC1 and BTFs are represented. (c) Genomic regions of *bona fide* BRC1 direct targets *BCH2* and *MAPKKK18*; in their promoters, BRC1 and BTFs binding sites overlap. (d) Genomic region of *BRC1*-dependent genes *4-HYDROXYPHENYLPYRUVATE DIOXYGENASE* (*HPD*) and *HISTONE 3.1* (*H3.1*). Their promoters are not bound by BRC1, but they are bound by all four BTFs, whose binding sites overlap. Red triangles indicate BRC1 binding motifs. Dark blue triangles indicate G-box motifs.

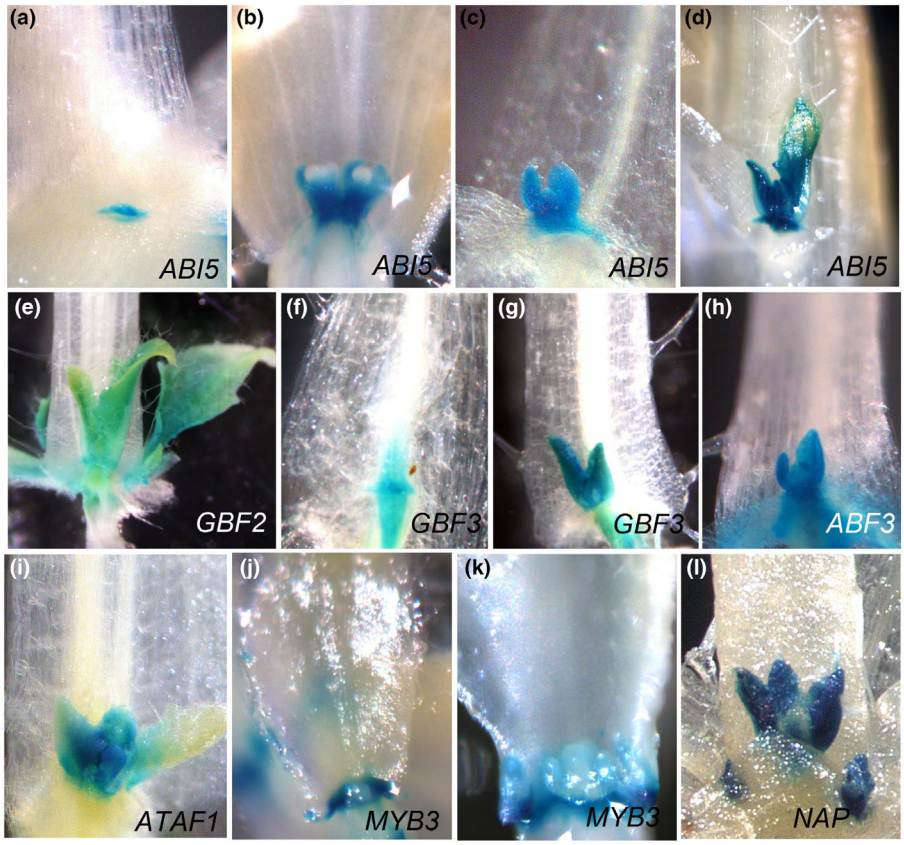

Fig. 6 BRC1 target genes encoding transcription factors (BTFs) are expressed in *Arabidopsis thaliana* axillary buds. *GUS* activity in axillary buds of transgenic lines *ABI5p::GUS* (a–d), *GBF2p::GUS* (e), *GBF3p::GUS* (f, g), *ABF3p::GUS* (h) and *ATAF1p::GUS* (i). The expression patterns of different BTFs are not identical: only *GBF3* and *ABF3* are expressed in the subtending vasculature. The expression of *MYB3* and *NAP*, BRANCHED1 (BRC1)-bound and *BRC1*-dependent genes, is also restricted to axillary buds as confirmed in *MYB3p::GUS* (j, k) and *NAPp::GUS* (l) transgenic lines. *MYB3* expression occurs at the base of the bud and is excluded from axillary meristems.

BTFs, namely ABF3 and ABI5 (Fig. S11). We fused each gene promoter to the CDS of the reporter gene *LUC* and conducted transient LUC assays in Nicotiana leaves. We co-infiltrated each *promoter::LUC* construct along with the oestradiol-inducible constructs *LEXA::BRC1*, *LEXA::ABI5*, *LEXA::ABF3* or with the combinations *LEXA::BRC1* + *LEXA::ABI5* or *LEXA::BRC1* + *LEXA::ABF3*, and measured the maximum LUC activity (Fig. 7).

All promoters were induced by BRC1 between 1.2 and 8.4 times relative to the controls, whereas none responded to either ABI5 or ABF3 alone. However, ABF3 significantly enhanced the response to BRC1 of the *HB53*, *MAPKKK18*, *BCH2* and *AT5G0522* promoters, and ABI5, the response of the *HB53* and *BCH2* promoters. By contrast, ABF3 reduced the response to BRC1 of the *ABI5* and *ATAF1* promoters, and ABI5 that of *SAG20*, *ABI5*, *ATAF1* and *GBF3*. These results indicate that some BTFs can modulate the transcriptional responses to BRC1.

Single BTF mutants have no or limited excess of branching

Finally, we tested the branching phenotype of mutants for two of the BTFs, specifically *ABI5* and *ABF3*. *abf3-cr1* plants grown for a month in short days and then transferred to long days, had a mild but significantly increased number of branches compared with the WT (Fig. S12). In contrast, *abi5-8* mutants did not display significant alterations in shoot branching. These results were consistent with the hypothesis that the BRC1 GRN is robust against mutation, and therefore, substantial effects from mutations in individual BTFs are not anticipated.

Discussion

By combining transcriptomic and BRC1 ChIP-Seq data from young seedlings with robust transcriptomic data from axillary buds (González-Grandío *et al.*, 2013), we have identified a collection of *bona fide* BRC1 direct targets. The biological significance of these candidate genes is supported by the significant enrichment of the *BRC1*-dependent gene clusters obtained in buds in genes from the lists of BRC1-bound and DEG genes identified in seedlings (Fig. S4). This substantial overlap between gene lists generated from independent analyses in different tissues provides strong support for the relevance of the proposed *bona fide* BRC1 direct target genes despite the fact that ectopic induction of *BRC1* in seedlings was used.

We show here that *BRC1* is a master regulator of a GRN that promotes bud dormancy in axillary buds. BRC1 directly controls the expression of a collection of BTFs that modulate and expand *BRC1* function, both by binding and influencing the response of some BRC1 direct targets and by regulating secondary *BRC1*-dependent genes not bound by BRC1.

One of the main mechanisms by which *BRC1* promotes dormancy is by induction of ABA signalling to cause growth arrest. We had previously shown that BRC1 directly regulates the expression of *HB21*, *HB40* and *HB53*, with in turn (together with *BRC1*) activate *NCED3*, an enzyme catalysing a rate-limiting step of ABA biosynthesis (González-Grandío *et al.*, 2017). Now, we demonstrate that BRC1 has a more pervasive influence on ABA signalling: a significant proportion of the *bona fide* BRC1 direct targets are involved in ABA metabolism, transport, perception, signalling and response. This enrichment in ABA-related targets has also been observed for maize TB1 (Dong *et al.*, 2019). Indeed, several common targets between TB1 and BRC1 are related to ABA (e.g. *HB53*/*HB40*, *ANAC032*, *ABF3*, *ABI5*, *NCED3* and *LEA4-5*). This suggests that the control of ABA signalling by BRC1/TB1 genes is evolutionary ancient and predates the separation of monocot and dicot plants. BRC1 may also induce GA degradation (via induction of *GA2OX2*), which would stabilise the growth-inhibiting DELLA proteins. Furthermore, BRC1 directly upregulates the SL biosynthesis gene *MAX1*. SL signalling boosts *BRC1* mRNA accumulation thus probably creating a positive regulatory FBL that bolsters *BRC1* responses and bud dormancy. In addition, BRC1 directly regulates a substantial number of transporters of signalling molecules, nutrients, ions and water. This may allow the bud to accurately assess the global energy and nutrient status of the plant, as well as confer resistance to hydric stress.

Our ChIP-Seq and RNA-Seq data show that BRC1 mainly acts as a transcriptional activator, which binds GDCCCA DNA motifs preferentially located in gene promoters, in close proximity to the TSS. Likewise, TB1 binds a related (although not identical) motif (GGnCCC) mainly in gene promoters (Dong *et al.*, 2019). However, the significant enrichment of G-box-like motifs (BACGTGKC) in relatively close proximity to BRC1 ChIP-Seq peaks, suggests that BRC1 targets are co-regulated by G-box-binding factors. Notably, ABA transcriptional networks are also enriched in G-box-containing ABA response elements (ABREs; Cutler *et al.*, 2010), and several BTFs (i.e. bZIP factors ABI5, GBF2, GBF3, ABF3, NAC factors ANAC032 and ATAF1) bind G-box motifs and are ABA master regulators (Cutler *et al.*, 2010; Fujita *et al.*, 2011; Song *et al.*, 2016). Furthermore, the specific gene targets and binding peaks of the BTFs significantly overlap with those of BRC1, which makes them likely candidates to have a critical impact on the *BRC1* transcriptional network. BRC1 and G-box-binding motifs are in some cases in close proximity, raising the possibility that BRC1 and BTFs physically interact, or that BRC1 increases chromatin accessibility of the BTFs to their targets in axillary buds, a tissue in which otherwise BTFs might not bind their targets.

Indeed, although *BRC1* expression is sufficient to activate BTFs and their downstream targets (González-Grandío *et al.*, 2017, this work), many of these genes belong to a well-characterised ABA network induced in seedlings where *BRC1* is not usually expressed (e.g. Lumba *et al.*, 2014; Song *et al.*, 2016). This raises the possibility that BRC1 has co-opted a pre-existing ABA signalling network to be activated in axillary buds under BRC1 control. This could have been achieved by acquisition of BRC1-binding sites at promoters of top-tier ABA master regulators to become BTFs (i.e. *ABI5*, *ABF3*, *GBF2*, *GBF3*, *ANAC032*, *HB21*, *HB40* and *HB53*), which in turn would activate other ABA-related targets, including other TFs. BRC1-binding sites evolved in secondary targets could generate FFLs between BRC1 and the BTFs. The observation that BRC1 is not induced by ABA treatments (González-Grandío *et al.*, 2017) and is not co-

expressed with ABA networks in other tissues, supports the view that BRC1 is an ABA-independent, master regulator of the ABA network, exclusively in buds. Some BTFs (e.g. ABF3, ABI5 and ATAF1) require ABA-induced phosphorylation for full activation (Fujita *et al.*, 2011). *BRC1*-mediated ABA biosynthesis (by upregulation of *BCH2* and *NCED3*) may be instrumental for this post-translational activation, and for additional support of the ABA-related responses.

The BRC1 GRN is enriched in multi-output FFLs (Alon, 2007) formed by BRC1, BTFs and other *bona fide* BRC1

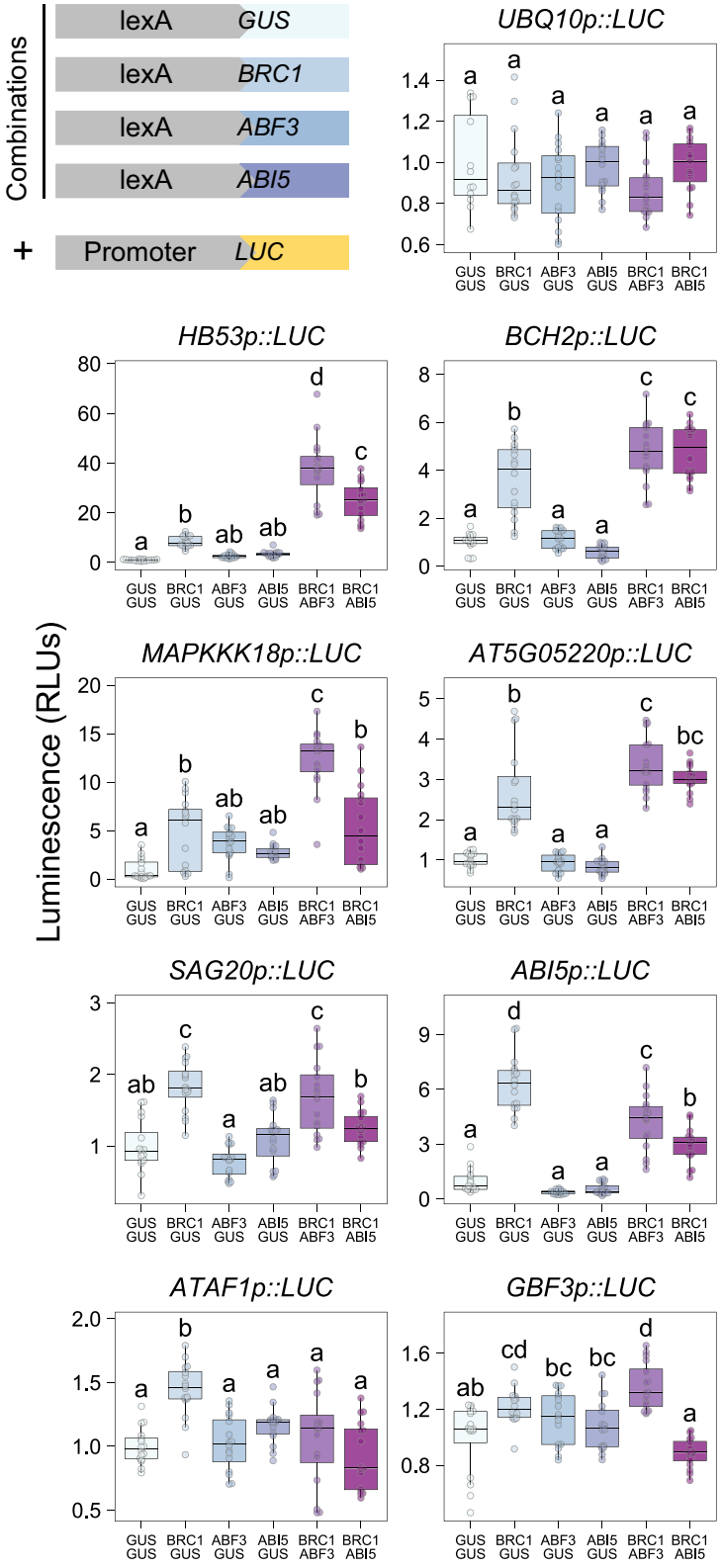

Fig. 7 *In vivo* validation of feed-forward loops (FFLs) involving BRANCHED1 (BRC1) and BRC1-targeted transcription factors (BTFs) ABF3 and ABI5. Schematic representation of constructs used for co-transfection assays. The promoters of eight *Arabidopsis thaliana* BRC1 *bona fide* direct targets fused to LUC were co-agroinfiltrated into *Nicotiana benthamiana* leaves with oestradiol-inducible *LEXA::BRC1*, *LEXA::ABF3*, *LEXA::ABI5* or their combinations. *LEXA::GUS* was co-infiltrated in single-gene experiments. *BRC1*-unresponsive *UBIQUITIN10::LUC* construct was assayed as a negative control. Luminescence is relative to the assay in which only *LEXA::GUS* and *promoter::LUC* fusion were infiltrated. Lower and upper hinges of the boxplot correspond to the first and third quartiles, upper and lower whiskers correspond to the largest value no further than 1.5 times the interquartile range. Statistical significance was determined by one-way ANOVA with *post hoc* Tukey HSD test. Letters denote significant differences among means ($n = 16$ for each plasmid combination).

targets. These type of network motifs are found in transcriptional networks in which environmental signals induce rapid and robust, but reversible, responses. They act as elements that sense and respond to persistent signals (Mine *et al.*, 2017; Joanito *et al.*, 2018). Thus, they could help filtering out signals that transiently induce *BRC1* expression, such as a brief shading, so that only persistent signals (e.g. a dense plant canopy) lead to network induction. Alternatively, they could cause a rapid and persistent response during a transient loss of *BRC1* induction. The BRC1 GRN is also enriched in multi-output FBLs formed by BTFs that regulate each other and jointly control downstream genes. These motifs provide memory of input signals and are commonly found in transcriptional networks that translate signals into stable decisions, such as developmental cell fates. In the BRC1 GRN, they could ensure that external or internal cues inducing *BRC1* are locked into steady-state responses that stabilise bud dormancy. The final output will depend on the prevailing network motifs, their sign (positive or negative), and additional, *BRC1*-independent regulation of network components. In addition, the BRC1 GRN is predicted to be robust against mutation, an essential feature to maintain a high fitness state. In line with this, mutations in single BTFs, such as *ABI5* and *ABF3*, display WT or mild branching phenotypes.

In summary, during the evolution of angiosperms, BRC1/TB1 genes seem to have recruited a highly connected ABA-related network comprising a collection of master regulators of ABA signalling and their targets. The flexibility of this network robust against noise and mutation, reversible in the first steps consisting of FFLs, but stable once stablished by FBLs, may be essential for an adaptive response and correct carbon allocation under growth-limiting conditions. This knowledge will prove fundamental to optimise plant architecture and crop production.

Acknowledgements

The research was supported by grants from the Dutch Scientific Organization (NWO) (NWO-JSTP grant 833.13.008 and VENI 15060), Spanish Ministry of Economy (MINECO) and fondos FEDER (PID2020-112779RB-I00/AEI/10.13039/501100011033, BIO2017-84363-R, BIO2017-84066-R and BIO2014-57011-R). CT was a La Caixa fellow and Aitor Muñoz-Gasca an FPI (MINECO) fellow PRE2018-083865, funded by MCIN/-AEI/10.13039/501100011033 and by ESF Invest in Your Future. We thank Juan Carlos Oliveros, Mónica Franch and F.J.M. van Workum for help with the RNA- and ChIP-Seq data analysis, Estíbaliz Bustos for amplification of BTF promoters and Javier Paz-Ares, Desmond Bradley, Monica Chagoyen and Juan Carlos Oliveros for constructive criticisms of the manuscript.

Competing interests

None declared.

Author contributions

PC, GCA and RGHI conceived and designed the research. SWvE, AM-G, EG-G and CT performed the experiments. PC, RGHI and GCA supervised the experiments. FJR-C, PdlR, ADJvD, WvE and AP-G analysed the data. PC and RGHI wrote the manuscript. SWvE and AM-G contributed equally to this work.

ORCID

Gerco C. Angenent https://orcid.org/0000-0003-4051-1078
Pilar Cubas https://orcid.org/0000-0003-4679-2173
Aalt D. J. van Dijk https://orcid.org/0000-0002-8872-5123
Sam W. van Es https://orcid.org/0000-0001-8042-3756
Wilma van Esse https://orcid.org/0000-0001-5012-2346
Eduardo González-Grandío https://orcid.org/0000-0002-2059-4542
Richard G. H. Immink https://orcid.org/0000-0002-0182-4138
Aitor Muñoz-Gasca https://orcid.org/0000-0002-9996-3426
Alberto Pascual-García https://orcid.org/0000-0002-8444-3196
Pedro de los Reyes https://orcid.org/0000-0002-7725-3087
Francisco J. Romero-Campero https://orcid.org/0000-0001-9834-030X

Data availability

The RNA-Seq data are available via NCBI and can be accessed through GEO accession no. GSE155028. The ChIP-Seq data are available via NCBI and can be accessed through GEO accession no. GSE155028. The R source code for this algorithm and the rest of scripts used for the construction and analysis of BRC1NET (https://greennetwork.us.es/BRC1NET) are available in the GitHub repository https://github.com/fran-romero-campero/BRC1NET.

References

Aguilar-Martínez JA, Poza-Carrión C, Cubas P. 2007. Arabidopsis BRANCHED1 acts as an integrator of branching signals within axillary buds. *Plant Cell* **19**: 458–472.

Alon U. 2007. Network motifs: theory and experimental approaches. *Nature Reviews Genetics* **8**: 450–461.

Bailey TL. 2011. DREME: motif discovery in transcription factor ChIP-seq data. *Bioinformatics* **27**: 1653–1659.

Bailey TL, Elkan C. 1994. Fitting a mixture model by expectation maximization to discover motifs in biopolymers. *Proceedings of the Second International Conference on Intelligent Systems for Molecular Biology* **2**: 28–36.

Bailey TL, MacHanick P. 2012. Inferring direct DNA binding from ChIP-seq. *Nucleic Acids Research* **40**: 1–10.

Barbier FF, Dun EA, Kerr SC, Chabikwa TG, Beveridge CA. 2019. An update on the signals controlling shoot branching. *Trends in Plant Science* **24**: 220–236.

Bencivenga S, Serrano-Mislata A, Bush M, Fox S, Sablowski R. 2016. Control of oriented tissue growth through repression of organ boundary genes promotes stem morphogenesis. *Developmental Cell* **39**: 198–208.

Booker J, Sieberer T, Wright W, Williamson L, Willett B, Stirnberg P, Turnbull C, Srinivasan M, Goddard P, Leyser O. 2005. MAX1 encodes a cytochrome P450 family member that acts downstream of MAX3/4 to produce a carotenoid-derived branch-inhibiting hormone. *Developmental Cell* **8**: 443–449.

Carstens CJ, Berger A, Strona G. 2018. A unifying framework for fast randomization of ecological networks with fixed (node) degrees. *MethodsX* **5**: 773–780.

Clough SJ, Bent AF. 1998. Floral dip: a simplified method for *Agrobacterium*-mediated transformation of *Arabidopsis thaliana*. *The Plant Journal* **16**: 735–743.

Coego A, Brizuela E, Castillejo P, Ruíz S, Koncz C, del Pozo JC, Piñeiro M, Jarillo JA, Paz-Ares J, León J *et al.* 2014. The TRANSPLANTA collection of Arabidopsis lines: a resource for functional analysis of transcription factors based on their conditional overexpression. *The Plant Journal* **77**: 944–953.

Cubas P, Vincent C, Coen E. 1999. An epigenetic mutation responsible for natural variation in floral symmetry. *Nature* **401**: 157–161.

Curtis M, Grossniklaus U. 2003. A gateway cloning vector set for high-throughput functional analysis of genes in planta. *Plant Physiology* **133**: 462–469.

Cutler SR, Rodriguez PL, Finkelstein RR, Abrams SR. 2010. Abscisic acid: emergence of a core signaling network. *Annual Review of Plant Biology* **61**: 651–679.

Dong Z, Xiao Y, Govindarajulu R, Feil R, Siddoway ML, Nielsen T, Lunn JE, Hawkins J, Whipple C, Chuck G. 2019. The regulatory landscape of a core maize domestication module controlling bud dormancy and growth repression. *Nature Communications* **10**: 3810.

Fujita Y, Fujita M, Shinozaki K, Yamaguchi-Shinozaki K. 2011. ABA-mediated transcriptional regulation in response to osmotic stress in plants. *Journal of Plant Research* **124**: 509–525.

Gidda SK, Miersch O, Levitin A, Schmidt J, Wasternack C, Varin L. 2003. Biochemical and molecular characterization of a hydroxyjasmonate sulfotransferase from *Arabidopsis thaliana*. *Journal of Biological Chemistry* **278**: 17895–17900.

González-Grandío E, Cubas P. 2015. Chapter 9. TCP transcription factors: evolution, structure, and biochemical function. In: Gonzalez DH, ed. *Plant transcription factors: evolutionary, structural and functional aspects*. Amsterdam, the Netherlands: Elsevier, 139–151.

González-Grandío E, Demirer GS, Ma W, Brady S, Landry MP. 2021. A ratiometric dual color luciferase reporter for fast characterization of transcriptional regulatory elements in plants. *ACS Synthetic Biology* **10**: 2763–2766.

González-Grandío E, Pajoro A, Franco-Zorrilla JM, Tarancon C, Immink RGH, Cubas P. 2017. Abscisic acid signaling is controlled by a BRANCHED1/HD-ZIP i cascade in Arabidopsis axillary buds. *Proceedings of the National Academy of Sciences, USA* **114**: E245–E254.

González-Grandío E, Poza-Carrión C, Sorzano COS, Cubas P. 2013. BRANCHED1 promotes axillary bud dormancy in response to shade in Arabidopsis. *Plant Cell* **25**: 834–850.

Joanito I, Chu JW, Wu SH, Hsu CP. 2018. An incoherent feed-forward loop switches the Arabidopsis clock rapidly between two hysteretic states. *Scientific Reports* **8**: 1–16.

Kaufmann K, Muiño JM, Jauregui R, Airoldi CA, Smaczniak C, Krajewski P, Angenent GC. 2009. Target genes of the MADS transcription factor SEPALLATA3: integration of developmental and hormonal pathways in the Arabidopsis flower. *PLoS Biology* **7**: e1000090.

Kaufmann K, Pajoro A, Angenent GC. 2010. Regulation of transcription in plants: mechanisms controlling developmental switches. *Nature Reviews Genetics* **11**: 830–842.

Kidder BL, Hu G, Zhao K. 2011. ChIP-Seq: technical considerations for obtaining high-quality data. *Nature Immunology* **12**: 918–922.

Kulkarni SR, Vaneechoutte D, Van de Velde J, Vandepoele K. 2018. TF2Network: predicting transcription factor regulators and gene regulatory networks in Arabidopsis using publicly available binding site information. *Nucleic Acids Research* **46**: e31.

Langmead B, Salzberg SL. 2012. Fast gapped-read alignment with Bowtie 2. *Nature Methods* **9**: 357–359.

Lumba S, Toh S, Handfield LF, Swan M, Liu R, Youn JY, Cutler SR, Subramaniam R, Provart N, Moses A *et al.* 2014. A mesoscale abscisic acid hormone interactome reveals a dynamic signaling landscape in Arabidopsis. *Developmental Cell* **29**: 360–372.

Machanick P, Bailey TL. 2011. Meme-ChIP: motif analysis of large DNA datasets. *Bioinformatics* **27**: 1696–1697.

Maere S, Heymans K, Kuiper M. 2005. Bingo: a Cytoscape plugin to assess overrepresentation of Gene Ontology categories in Biological Networks. *Bioinformatics* **21**: 3448–3449.

Martín-Fontecha ES, Tarancón C, Cubas P. 2018. To grow or not to grow, a power-saving program induced in dormant buds. *Current Opinion in Plant Biology* **41**: 102–109.

Maurya JP, Singh RK, Miskolczi PC, Prasad AN, Jonsson K, Wu F, Bhalerao RP. 2020. Branching regulator BRC1 mediates photoperiodic control of seasonal growth in hybrid aspen. *Current Biology* **30**: 122–126.

Menkens AE, Schindler U, Cashmore AR. 1995. The G-box: a ubiquitous regulatory DNA element in plants bound by the GBF family of bZIP proteins. *Trends in Biochemical Sciences* **20**: 506–510.

Mi H, Huang X, Muruganujan A, Tang H, Mills C, Kang D, Thomas PD. 2017. Panther v.11: expanded annotation data from Gene Ontology and Reactome pathways, and data analysis tool enhancements. *Nucleic Acids Research* **45**: D183–D189.

Milo R, Shen-Orr S, Itzkovitz S, Kashtan N, Chklovskii D, Alon U. 2002. Network motifs: simple building blocks of complex networks. *Science* **298**: 824–827.

Mine A, Nobori T, Salazar-Rondon MC, Winkelmüller TM, Anver S, Becker D, Tsuda K. 2017. An incoherent feed-forward loop mediates robustness and tunability in a plant immune network. *EMBO Reports* **18**: 464–476.

van Mourik H, Muiño JM, Pajoro A, Angenent GC, Kaufmann K. 2015. Characterization of *in vivo* DNA-binding events of plant transcription factors by ChIP-seq: experimental protocol and computational analysis. *Methods in Molecular Biology* **1284**: 93–121.

Muiño JM, Kaufmann K, van Ham RC, Angenent GC, Krajewski P. 2011. ChIP-seq analysis in R (csar): an R package for the statistical detection of protein-bound genomic regions. *Plant Methods* **7**: 11.

Nakagawa T, Suzuki T, Murata S, Nakamura S, Hino T, Maeo K, Tabata R, Kawai T, Tanaka K, Niwa Y *et al.* 2007. Improved gateway binary vectors: high-performance vectors for creation of fusion constructs in transgenic analysis of plants. *Bioscience, Biotechnology and Biochemistry* **71**: 2095–2100.

Obayashi T, Aoki Y, Tadaka S, Kagaya Y, Kinoshita K. 2018. ATTED-II in 2018: a plant coexpression database based on investigation of the statistical property of the mutual rank index. *Plant and Cell Physiology* **59**: E3.

Obayashi T, Kinoshita K, Nakai K, Shibaoka M, Hayashi S, Saeki M, Shibata D, Saito K, Ohta H. 2007. ATTED-II: a database of co-expressed genes and cis elements for identifying co-regulated gene groups in Arabidopsis. *Nucleic Acids Research* **35**: 4–6.

O'Malley RC, Huang SS-C, Song L, Lewsey MG, Bartlett A, Nery JR, Galli M, Gallavotti A, Ecker JR. 2016. Erratum: Cistrome and epicistrome features

shape the regulatory DNA landscape (Cell (2016) 165(5) (1280–1292)). *Cell* **166**: 1598.

Ran X, Zhao F, Wang Y, Liu J, Zhuang Y, Ye L, Qi M, Cheng J, Zhang Y. 2020. Plant regulomics: a data-driven interface for retrieving upstream regulators from plant multi-omics data. *The Plant Journal* **101**: 237–248.

Ruggiero B, Koiwa H, Manabe Y, Quist TM, Inan G, Saccardo F, Joly RJ, Hasegawa PM, Bressan RA, Maggio A. 2004. Uncoupling the effects of abscisic acid on plant growth and water relations. Analysis of sto1/nced3, an abscisic acid-deficient but salt stress-tolerant mutant in Arabidopsis. *Plant Physiology* **136**: 3134–3147.

Sessions A, Weigel D, Yanofsky MF. 1999. The *Arabidopsis thaliana* MERISTEM LAYER 1 promoter specifies epidermal expression in meristems and young primordia. *The Plant Journal* **20**: 259–263.

Shannon P, Markiel A, Ozier O, Baliga NS, Wang JT, Ramage D, Amin N, Schwikowski B, Ideker T. 2003. CYTOSCAPE: a software environment for integrated models of biomolecular interaction networks. *Genome Research* **13**: 2498–2504.

Song L, Huang SSC, Wise A, Castanoz R, Nery JR, Chen H, Watanabe M, Thomas J, Bar-Joseph Z, Ecker JR. 2016. A transcription factor hierarchy defines an environmental stress response network. *Science* **354**: aag1550.

Świątek A, Lenjou M, Van Bockstaele D, Inzé D, Van Onckelen H. 2002. Differential effect of jasmonic acid and abscisic acid on cell cycle progression in tobacco BY-2 cells. *Plant Physiology* **128**: 201–211.

Trapnell C, Roberts A, Goff L, Pertea G, Kim D, Kelley DR, Pimentel H, Salzberg SL, Rinn JL, Pachter L. 2012. Differential gene and transcript expression analysis of RNA-seq experiments with TOPHAT and CUFFLINKS. *Nature Protocols* **7**: 562–578.

Vazquez-Vilar M, Quijano-Rubio A, Fernandez-Del-Carmen A, Sarrion-Perdigones A, Ochoa-Fernandez R, Ziarsolo P, Blanca J, Granell A, Orzaez D. 2017. GB3.0: a platform for plant bio-design that connects functional DNA elements with associated biological data. *Nucleic Acids Research* **45**: 2196–2209.

Wang M, Le Moigne MA, Bertheloot J, Crespel L, Perez-Garcia MD, Ogé L, Demotes-Mainard S, Hamama L, Davière JM, Sakr S. 2019. BRANCHED1: a key hub of shoot branching. *Frontiers in Plant Science* **10**: 1–12.

Yang X, Yan J, Zhang Z, Lin T, Xin T, Wang B, Wang S, Zhao J, Zhang Z, Lucas WJ *et al.* 2020. Regulation of plant architecture by a new histone acetyltransferase targeting gene bodies. *Nature Plants* **6**: 809–822.

Zhang Y, Liu T, Meyer CA, Eeckhoute J, Johnson DS, Bernstein BE, Nussbaum C, Myers RM, Brown M, Li W *et al.* 2008. Model-based analysis of ChIP-Seq (MACS). *Genome Biology* **9**: R137.

Zheng Y, Schumaker KS, Guo Y. 2012. Sumoylation of transcription factor MYB30 by the small ubiquitin-like modifier E3 ligase SIZ1 mediates abscisic acid response in *Arabidopsis thaliana*. *Proceedings of the National Academy of Sciences, USA* **109**: 12822–12827.

Supporting Information

Additional Supporting Information may be found online in the Supporting Information section at the end of the article.

Dataset S1 Primer list.

Dataset S2 Co-expression Clusters and GO enrichment.

Dataset S3 BRC1-bound genes.

Dataset S4 BRC1-responsive genes.

Dataset S5 Bona fide BRC1 targets.

Dataset S6 Predicted regulators of the BRC1 network.

Dataset S7 Network motifs.

Fig. S1 Schematic representation of the steps followed to identify *bona fide* BRC1 direct targets.

Fig. S2 Validation of co-expressed gene clusters.

Fig. S3 Analysis of BRC1 ChIP-Seq datasets.

Fig. S4 UP BRC1-dependent clusters are enriched in BRC1 direct targets.

Fig. S5 Motifs enriched in the binding sites of BTFs indicated.

Fig. S6 Screenshots of the BRC1NET web application.

Fig. S7 ABF3 targets in the BRC1 network are significantly enriched in UP_C1 genes.

Fig. S8 Network motifs identified in the transcriptional network downstream of BRC1.

Fig. S9 Common targets of ABI5 and ANAC032 are significantly enriched in genes from UP_C6.

Fig. S10 BRC1 network is robust against mutation.

Fig. S11 Mapping of the BRC1, ABF3 and ABI5 binding sites in several BRC1 direct targets.

Fig. S12 Branching phenotype of BTF mutants.

Notes S1 Comparison of *Arabidopsis thaliana* BRC1 and *Zea mays* TB1 downstream targets.

Table S1 Overview of significantly overrepresented motifs in BRC1 ChIP-Seq peaks.

Table S2 Significance analysis of overlap between BTF targets and genes of each *BRC1*-dependent cluster.

Table S3 Enrichment analysis of BTF targets in genes of each BRC1-dependent cluster.

Table S4 Significance analysis of the contribution of FBLs to the regulation of the *BRC1*-dependent genes.

Table S5 Contribution of FBLs to the regulation of the *BRC1*-dependent genes.

Please note: Wiley is not responsible for the content or functionality of any Supporting Information supplied by the authors. Any queries (other than missing material) should be directed to the *New Phytologist* Central Office.